Inorg. Chem. **2008**, *47*, 5177−5183

Inorganic Chemistry
Article

Use of Bifunctional Phosphonates for the Preparation of Heterobimetallic 5f−3d Systems

Andrea N. Alsobrook, Wei Zhan, and Thomas E. Albrecht-Schmitt*

A Contribution from the Department of Chemistry and Biochemistry and Center for Actinide Science, Auburn University, Auburn, Alabama 36849

Received January 30, 2008

The hydrothermal reaction of phosphonoacetic acid ($H_2PO_3CH_2C(O)OH$, **PAA**) with UO_3 and $Cu(C_2H_3O_2)_2 \cdot H_2O$ results in the formation of the crystalline heterobimetallic uranium(VI)/copper(II) phosphonates $UO_2Cu(PO_3CH_2CO_2)(OH)(H_2O)_2$ (**UCuPAA-1**), $(UO_2)_2Cu(PO_3CH_2CO_2)_2(H_2O)_3$ (**UCuPAA-2**), and $[H_3O][(UO_2)_2Cu_2(PO_3CH_2CO_2)_3(H_2O)_2$ (**UCuPAA-3**). The addition of sodium hydroxide to the aforementioned reactions results in the formation of $Na[UO_2(PO_3CH_2CO_2)] \cdot 2H_2O$ (**NaUPAA-1**). These compounds display 1D (**UCuPAA-1**), 2D (**UCuPAA-2**, **NaUPAA-1**), and 3D (**UCuPAA-3**) architectures wherein the phosphonate portion of the ligand primarily coordinates the uranium(VI) centers; whereas the carboxylate moiety preferentially, but not exclusively, binds to the copper(II) ions. Fluorescence measurements on all four compounds demonstrate that the presence of copper(II) mostly quenches the emission from the uranyl moieties.

Introduction

Bifunctional phosphonates have been the subject of intense recent interest because of the ability of these ligands to tune the properties of materials. A variety of multifunctional phosphonates have been developed that include those with amine, hydroxyl, carboxylate, crown-ether, N-oxide, or sulfonate moieties.[1] Metal complexes of bifunctional phosphonates have potential applications in a wide variety of areas including proton conductivity, ion-exchange, sensing, separations, and catalysis.[1] Of late, we have been investigating new actinide phosphonate materials primarily from the perspective of developing magneto-structural correlations.[2] The use of bifunctional phosphonates, as we will show in this work, allows for the preparation of 5f−3d systems that are of interest for both structural and electronic reasons.

The solid-state chemistry of actinide phosphonates has been partially developed with thorium[3] and uranium[4,5] and to a very limited extent with neptunium.[2] Structural data on thorium phosphonates has been inferred from powder X-ray diffraction experiments.[3] However, both high-resolution powder diffraction data and extensive single crystal X-ray diffraction data are available for uranium(VI) phosphonates.[4] Whereas a structure has been deduced for a single uranium(IV) phosphonate,[5] little is known about tetravalent actinide phosphonates.[2]

Currently, considerable attention is being paid to investigating the electronic coupling of heterometallic f−d compounds, with a strong focus on obtaining systems with magnetic coupling between the different metal centers. A number of divergent routes to compounds of this type have been developed that contain uranium and a transition metal.[6] The center of attention has been placed on obtaining uranium(IV) centers that are electronically coupled with unpaired electrons on transition metal ions.[6] One deleterious aspect of this that has been generally overlooked is that, while using a Russell−Saunders scheme a $^3H_4$ state is predicted

---

* To whom correspondence should be addressed. E-mail: albreth@auburn.edu.

(1) Clearfield, A. *Prog. Inorg. Chem.* **1998**, *47*, 371. Clearfield, A. *Curr. Opin. Solid State Mater. Sci.* **2003**, *6*, 495. Mao, J.-G. *Coord. Chem. Rev.* **2007**, *251*, 1493.

(2) Bray, T. H.; Nelson, A.-G. D.; Jin, G. B.; Haire, R. G.; Albrecht-Schmitt, T. E. *Inorg. Chem.* **2007**, *46*, 10959.

(3) Dines, M. B.; DiGiacomo, P. M. *Inorg. Chem.* **1981**, *20*, 92.

(4) Grohol, D.; Clearfield, A. *J. Am. Chem. Soc.* **1997**, *119*, 9301. Grohol, D.; Clearfield, A. *J. Am. Chem. Soc.* **1997**, *119*, 4662. Grohol, D.; Subramanian, M. A.; Poojary, D. M.; Clearfield, A. *Inorg. Chem.* **1996**, *35*, 5264. Poojary, D. M.; Cabeza, A.; Aranda, M. A. G.; Bruque, S.; Clearfield, A. *Inorg. Chem.* **1996**, *35*, 5603. Poojary, D. M.; Grohol, D.; Clearfield, A. *Angew. Chem., Int. Ed. Engl.* **1995**, *34*, 1508. Poojary, D. M.; Grohol, D.; Clearfield, A. *J. Phys. Chem. Solids* **1995**, *56*, 1383. Britel, A.; Wozniak, M.; Boivin, J. C.; Nowogrocki, G.; Thomas, D. *Acta Crystallogr.* **1986**, *C42*, 1502. Grohol, D.; Clearfield, A. *Inorg. Chem.* **1999**, *38*, 751. Doran, M. B.; Norquist, A. J.; O'Hare, D. *Chem. Mater.* **2003**, *15*, 1449. Bao, S.-S.; Chen, G.-S.; Wang, Y.; Li, Y.-Z.; Zheng, L.-M.; Luo, Q.-H. *Inorg. Chem.* **2006**, *45*, 1124.

(5) Cabeza, A.; Aranda, M. A. G.; Cantero, F. M.; Lozano, D.; Martínez-Lara, Bruque, S. *J. Solid State Chem.* **1996**, *121*, 181.

10.1021/ic800192r CCC: $40.75

Table 1. Crystallographic Data for $UO_2Cu(PO_3CH_2CO_2)(OH)(H_2O)_2$ (**UCuPAA-1**), $(UO_2)_2Cu(PO_3CH_2CO_2)_2(H_2O)_3$ (**UCuPAA-2**), $[H_3O][(UO_2)_2Cu_2(PO_3CH_2CO_2)_3(H_2O)_2]$ (**UCuPAA-3**), and $Na[UO_2(PO_3CH_2CO_2)]\cdot 2H_2O$ (**NaUPAA-1**)

compound	UCuPAA-1	UCuPAA-2	UCuPAA-3	NaUPAA-1
fw	518.58	925.61	1126.18	462.03
color and habit	dark green, tablet	light green, tablet	yellow, tablet	pale yellow, tablet
space group	$P2_1/c$ (No. 14)	$P2_1/c$ (No. 14)	$P\bar{1}$ (No. 2)	$P\bar{1}$ (No. 2)
a (Å)	6.9671(6)	7.6358(5)	8.8127(6)	6.8742(4)
b (Å)	14.2308(13)	19.3001(12)	10.0229(7)	7.4167(5)
c (Å)	9.0581(8)	11.2452(7)	14.7301(10)	9.6353(6)
α (deg)	90	90	83.4360	79.145(1)
β (deg)	98.390(2)	100.586(1)	83.9460	78.685(1)
γ (deg)	90	90	64.8680	63.886(1)
V(Å)	888.48(14)	1629.02(18)	1167.85(14)	429.62(5)
Z	4	4	2	2
T (K)	193	295	193	193
λ (Å)	0.71073	0.71073	0.71073	0.71073
ρ_{calcd} (g cm^{-3})	3.877	3.774	3.203	3.572
μ (Mo Kα) (cm^{-1})	208.17	214.12	159.23	191.53
$R(F)$ for $F_o^2 > 2\sigma(F_o^2)^a$	0.0349	0.0298	0.0540	0.0236
$R_w(F_o^2)^b$	0.0826	0.0753	0.1416	0.0638

[a] $R(F) = \sum||F_o| - |F_c|| / \sum|F_o|$. [b] $R_w(F_o^2) = [\sum[w(F_o^2 - F_c^2)^2]/\sum wF_o^4]^{1/2}$.

for uranium(IV),[7] at low temperatures a nonmagnetic singlet state is often obtained.[8] If a nonmagnetic ground-state is to be avoided, then neptunium is the element of choice, offering stable +4, +5, and +6 oxidation states, each offering its own unique possibilities for obtaining magnetically coupled systems. In this regard, we must begin these studies with model complexes containing uranium. Herein, we disclose that heterobimetallic uranium(VI)/copper(II) crystalline solids can be obtained by employing the bifunctional phosphonate, phosphonoacetic acid.

Experimental Section

Syntheses. UO_3 (98%, Strem), phosphonoacetic acid (H_2PO_3-$CH_2C(O)OH$, **PAA**) (98%, Alfa Aesar), and copper(II) acetate monohydrate (analytical grade, Mallinckrodt) were used as received. Reactions were run in PTFE-lined Parr 4749 autoclaves with a 23 mL internal volume. Distilled and Millipore filtered water with a resistance of 18.2 MΩ·cm was used in all reactions. Standard precautions were performed for handling radioactive materials during work with UO_3 and the products of the reactions. Semiquantitative EDX analyses were performed using a JEOL 7000F field emission SEM and confirmed the presence of the appropriate heavy elements in these compounds (U, Cu, P).

$UO_2Cu(PO_3CH_2CO_2)(OH)(H_2O)_2$ (UCuPAA-1), $(UO_2)_2Cu(PO_3CH_2CO_2)_2(H_2O)_3$(UCuPAA-2),$[H_3O][(UO_2)_2Cu_2(PO_3CH_2CO_2)_3(H_2O)_2$ (UCuPAA-3), and $Na[UO_2(PO_3CH_2CO_2)]\cdot 2H_2O$ (NaUPAA-1). UO_3 (200 mg, 0.699 mmol), phosphonoacetic acid (140 mg, 1.000 mmol), $Cu(C_2H_3O_2)_2\cdot H_2O$ (200 mg, 1 mmol), and 3 mL of water were loaded into a 23 mL autoclave. The autoclave was sealed and heated to 180 °C in a box furnace for 5 days. The autoclave was then cooled at an average rate of 9 °C/h to 35 °C. The product consisted of dark-green and light-green tablets of **UCuPAA-1** and **UCuPAA-2**, respectively. By increasing the reaction temperature to 200 °C and holding all other variables constant, **UCuPAA-3** is also obtained in the mixture. The addition of 233 μL of 0.1 M NaOH to the above starting reaction mixture adjusts the starting pH from 2.73 to 3.43 and results in the isolation of **NaUPAA-1**. The products were thoroughly washed with water, then rinsed with methanol, and allowed to dry.

Crystallographic Studies. Single crystals of $UO_2Cu(PO_3CH_2CO_2)(OH)(H_2O)_2$ (**UCuPAA-1**), $(UO_2)_2Cu(PO_3CH_2CO_2)_2(H_2O)_3$ (**UCuPAA-2**), $[H_3O][(UO_2)_2Cu_2(PO_3CH_2CO_2)_3(H_2O)_2$ (**UCuPAA-3**), and $Na[UO_2(PO_3CH_2CO_2)]\cdot 2H_2O$ (**NaUPAA-1**) were mounted on glass fibers, and optically aligned on a Bruker APEX CCD X-ray diffractometer using a digital camera. Initial intensity measurements were performed using graphite monochromated Mo Kα ($\lambda = 0.71073$ Å) radiation from a sealed tube and monocapillary collimator. *SMART* (ver. 5.624) was used for preliminary determination of the cell constants and data collection control. The intensities of reflections of a sphere were collected by a combination of 3 sets of exposures (frames). Each set had a different ϕ angle for the crystal, and each exposure covered a range of 0.3° in ω. A total of 1800 frames were collected with an exposure time per frame of 30 to 60 s, depending on the crystal.

For these compounds, determination of integrated intensities and global refinement were performed with the Bruker *SAINT* (ver. 6.02) software package using a narrow-frame integration algorithm. A numerical, face-indexed absorption correction was applied using *XPREP*.[9] The data were treated with a semiempirical absorption correction by *SADABS*.[10] The program suite *SHELXTL* (ver. 6.12) was used for space group determination (*XPREP*), direct methods structure solution (XS), and least-squares refinement (XL).[9] The final refinements included anisotropic displacement parameters for all atoms. Secondary extinction was not noted. Some crystallographic details are given in Table 1. Additional details can be found in the Supporting Information.

---

(6) Cramer, R. E.; Higa, K. T.; Pruskin, S. L.; Gilje, J. W. *J. Am. Chem. Soc.* **1983**, *105*, 6749. Day, V. W.; Klemperer, W. G.; Maltbie, D. J. *Organometallics* **1985**, *4*, 104. Cendrowski-Guillaume, S. M.; Lance, M.; Nierlich, M.; Vigner, J.; Ephritikhine, M. *J. Chem. Soc., Chem. Commun.* **1994**, 1665. Odom, A. L.; Arnold, P. L.; Cummins, C. C. *J. Am. Chem. Soc.* **1998**, *120*, 5836. Evans, W. J.; Nyce, G. W.; Greci, M. A.; Ziller, J. W. *Inorg. Chem.* **2001**, *40*, 6725. Sarsfield, M. J.; Sutton, A. D.; May, I.; John, G. H.; Sharrad, C.; Helliwell, M. *Chem. Commun.* **2004**, 2320. Arnold, P. L.; Patel, D.; Blake, A. J.; Wilson, C.; Love, J. B. *J. Am. Chem. Soc.* **2006**, *128*, 9610. Monreal, M. J.; Carver, C. T.; Diaconescu, P. L. *Inorg. Chem.* **2007**, *46*, 7226. Kozimor, S. A.; Bartlett, B. M.; Rinehart, J. D.; Long, J. R. *J. Am. Chem. Soc.* **2007**, *129*, 10672.

(7) Edelstein, N. M.; Lander, G. H. In *The Chemistry of the Actinide and Transactinide Elements*; Morss L., Edelstein N. M., Fuger J., Ed.; Springer: Dordrecht, 2006; Ch. 20.

(8) Almond, P. M.; Deakin, L.; Porter, M. O.; Mar, A.; Albrecht-Schmitt, T. E. *Chem. Mater.* **2000**, *12*, 3208. Schelter, E. J.; Morris, D. E.; Scott, B. L.; Thompson, J. D.; Kiplinger, J. L. *Inorg. Chem.* **2007**, *46*, 5528. Kiplinger, J. L.; Pool, J. A.; Schelter, E. J.; Thompson, J. D.; Scott, B. L.; Morris, D. E. *Angew. Chem., Int. Ed.* **2006**, *45*, 2036.

(9) Sheldrick, G. M. *SHELXTL PC, Version 6.12, An Integrated System for Solving, Refining, and Displaying Crystal Structures from Diffraction Data*; Siemens Analytical X-Ray Instruments, Inc.: Madison, WI 2001.

Fluorescence Spectroscopy. Fluorescence emission spectra of the single crystals were acquired using a PI Acton spectrometer (SpectraPro SP 2356, Acton, NJ) that is connected to the side port of an epi-fluorescence microscope (Nikon TE-2000U, Japan). The emission signal was recorded by a back-illuminated digital CCD camera (PI Acton PIXIS:400B, Acton, NJ) operated by a PC. For all the three compounds examined, the excitation was generated by a mercury lamp (X-Cite 120, EXFO, Ontario, Canada) filtered by a band-pass filter at 450−490 nm. The emission signal was filtered by a long-pass filter with a cutoff wavelength of 515 nm. The intensities of the spectra of the four compounds are not directly comparable to each other because different acquisition times and objective lenses were used.

Raman Spectroscopy. Raman spectra for all four compounds were collected from single crystals of each compound using a Renishaw inVia Confocal Raman microscope with a 514 nm Ar^+ laser.

Results and Discussion

Synthesis. The hydrothermal reaction of phosphonoacetic acid with UO_3 and $Cu(C_2H_3O_2)_2 \cdot H_2O$ results in the crystallization $UO_2Cu(PO_3CH_2CO_2)(OH)(H_2O)_2$ (**UCuPAA-1**), $(UO_2)_2Cu(PO_3CH_2CO_2)_2(H_2O)_3$ (**UCuPAA-2**), and $[H_3O][(UO_2)_2Cu_2(PO_3CH_2CO_2)_3(H_2O)_2]$ (**UCuPAA-3**). Of these compounds, only **UCuPAA-2** can be prepared directly as a reasonably pure phase; the others must be manually separated from one another on the basis of crystal color and morphology. In an attempt to obtain pure phases, the pH of the starting solution was adjusted using 0.1 M NaOH. However, this did not yield the desired result, and instead the copper-free uranyl phosphonate, $Na[UO_2(PO_3CH_2CO_2)] \cdot 2H_2O$ (**NaUPAA-1**), is isolated.

Structure of $UO_2Cu(PO_3CH_2CO_2)(OH)(H_2O)_2$ (UCuPAA-1). The structures of **UCuPAA-1**, **UCuPAA-2**, and **UCuPAA-3** are arranged in order of increasing complexity. The results of the single crystal X-ray diffraction experiments on **UCuPAA-1** revealed a 1D structure consisting of uranyl, UO_2^{2+}, cations bound by both the phosphonate and carboxylate portions of the phosphonoacetate ligand, as well as one hydroxide, as is shown in Figure 1. This results in a pentagonal bipyramidal environment around the uranium(VI) center. The uranyl U═O bonds are 1.785(7) and 1.789(6) Å; whereas those in the equatorial plane are longer and range from 2.305(6) to 2.572(6) Å. While the uranyl bond distances are quite typical for a uranium(VI) compound, bond-valence sum calculations that incorporate all of the inner-sphere interactions yield a value of 5.92 for uranium(1), which is entirely consistent with uranium(VI).[11] The UO_7 pentagonal bipyramid shares an edge with a roughly planar square containing the copper center. The Cu−O bonds range from 1.878(6) to 1.983(6) Å. Again bond-valence sums reveal the formal oxidation state of the copper as +2 with a value of 1.98.[12] Two of the Cu−O bonds are terminal and are assumed, based on both bond-length and charge-balance considerations, to be water molecules. Selected bond distances and angles for **UCuPAA-1** can be found in Table 2.

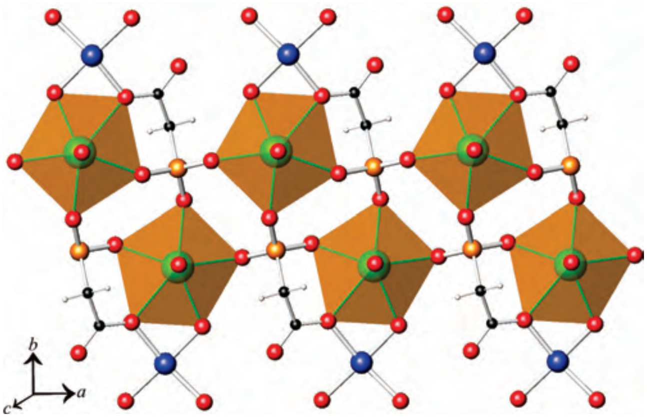

Figure 1. A view of part of the structure of $UO_2Cu(PO_3CH_2CO_2)(OH)(H_2O)_2$ (**UCuPAA-1**) showing 1D ribbons consisting of uranyl, UO_2^{2+}, cations bound by both the phosphonate and carboxylate portions of the phosphonoacetate ligand, as well as one hydroxide. The edges of the ribbons are terminated by square planar copper(II). UO_7 pentagonal bipyramids = orange, oxygen atoms = red, copper = blue, phosphorus = yellow, carbon = black, hydrogen = white.

Table 2. Selected Bond Distances (Angstroms) and Angles (Degrees) for $UO_2Cu(PO_3CH_2CO_2)(OH)(H_2O)_2$ **(UCuPAA-1)**

Distances (Angstroms)			
U(1)−O(6)	1.785(7)	Cu(1)−O(10)	1.951(6)
U(1)−O(7)	1.789(6)	Cu(1)−O(5)	1.983(6)
U(1)−O(8)	2.305(6)	P(1)−O(1)	1.513(6)
U(1)−O(1)	2.317(6)	P(1)−O(2)	1.530(6)
U(1)−O(3)	2.358(6)	P(1)−O(3)	1.532(6)
U(1)−O(2)	2.380(6)	P(1)−C(2)	1.801(9)
U(1)−O(5)	2.572(6)	C(1)−O(4)	1.233(10)
Cu(1)−O(8)	1.878(6)	C(1)−O(5)	1.302(10)
Cu(1)−O(9)	1.951(6)	C(1)−C(2)	1.518(11)

Angles (Degrees)			
O(6)−U(1)−O(7)	177.3(3)	O(10)−Cu(1)−O(5)	96.4(2)
O(8)−Cu(1)−O(10)	177.6(3)	O(9)−Cu(1)−O(5)	165.3(3)
O(8)−Cu(1)−O(9)	90.2(3)	O(8)−Cu(1)−O(7)	91.9(2)
O(10)−Cu(1)−O(9)	91.4(2)	O(10)−Cu(1)−O(7)	86.2(2)
O(8)−Cu(1)−O(5)	82.4(2)	O(9)−Cu(1)−O(7)	94.0(2)
O(5)−Cu(1)−O(7)	98.9(2)		

Structure of $(UO_2)_2Cu(PO_3CH_2CO_2)_2(H_2O)_3$ (UCuPAA-2). The structure of **UCuPAA-2** is layered and highly complex. Each layer contains two crystallographically unique uranium centers, both of which are found as UO_7 pentagonal bipyramids as found in **UCuPAA-1**. These units share a single corner to form a dimer. The average U═O bond length in the uranyl units is 1.779(5) Å, and the equatorial U−O bonds range from 2.261(4) to 2.682(4) Å. The bond-valence sums for U(1) and U(2) are 5.98 and 6.05, both of which are consistent with uranium(VI).[11] The phosphonoacetate trianions display two different bonding modes in the layers. One of these anions uses all five oxygen atoms to coordinate uranium(VI), binding a total of four uranium centers. The second anion uses four of its five oxygen atoms to bond to a total of four uranyl units. However, it leaves a single oxygen atom from the carboxylate portion of the anion pointing approximately perpendicular to the layers. This oxygen atom coordinates a $[Cu(H_2O)_3]^{2+}$ moiety creating a distorted square planar environment around the copper center with Cu−O bonds ranging from 1.949(5) to 1.982(5) Å. The

---

(10) Sheldrick, G. M. *Acta Crystallogr.* **1995**, *A51*, 33. . *SADABS* 2001, Program for absorption correction using SMART CCD based on the method of Blessing: Blessing, R. H

(11) Burns, P. C.; Ewing, R. C.; Hawthorne, F. C. *Can. Mineral.* **1997**, *35*, 1551.

(12) Brown, I. D.; Altermatt, D. *Acta Crystallogr.* **1985**, *B41*, 244. Brese, N. E.; O'Keeffe, M. *Acta Crystallogr.* **1991**, *B47*, 192.

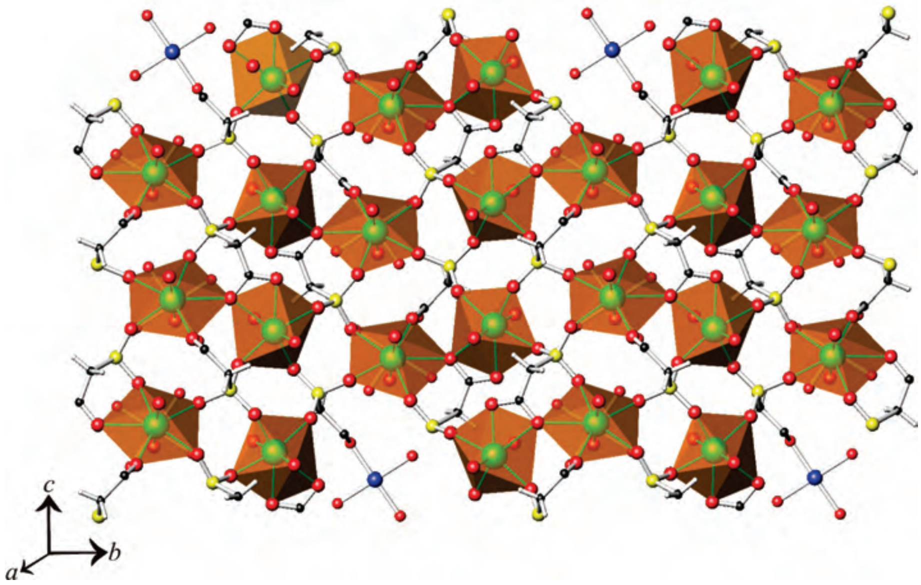

Figure 2. A depiction of part of a corrugated layer found in $(UO_2)_2Cu(PO_3CH_2CO_2)_2(H_2O)_3$ (**UCuPAA-2**) in the [*bc*] plane. UO_7 pentagonal bipyramids = orange, oxygen atoms = red, copper = blue, phosphorus = yellow, carbon = black, hydrogen = white.

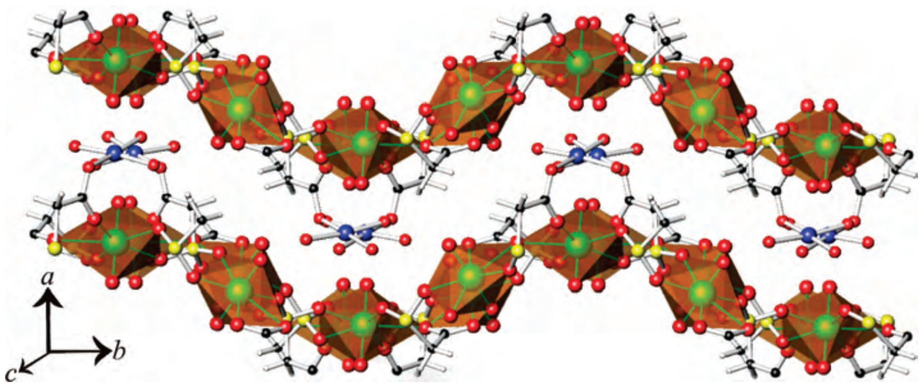

Figure 3. An illustration of the stacking of the layers along the *a* axis for $(UO_2)_2Cu(PO_3CH_2CO_2)_2(H_2O)_3$ (**UCuPAA-2**). UO_7 pentagonal bipyramids = orange, oxygen atoms = red, copper = blue, phosphorus = yellow, carbon = black, hydrogen = white.

bond-valence sum for the copper ion is 1.86, and as found for **UCuPAA-1**, this value is consistent with copper(II).[12] These CuO_4 units extend in between the layers. A view of part of a corrugated layer in the [*bc*] plane is shown in Figure 2, and the stacking of these layers along the *a* axis is depicted in Figure 3. Selected bond distances and angles for **UCuPAA-2** can be found in Table 3.

Structure of $[H_3O][(UO_2)_2Cu_2(PO_3CH_2CO_2)_3(H_2O)_2$ (UCuPAA-3). The structure of **UCuPAA-3** is the most complex of the four compounds described in this work. A reflection of this complexity is the presence of two distinct uranyl moieties and three different copper centers. The overall structure is 3D. However, there are lower-dimensional features that can be used to describe the architecture of this compound in better detail. By referring to Figure 4, it can be seen that there are layered features within the 3D framework. As found in **UCuPAA-2**, there are corner-sharing UO_7 dimers. Again all evidence points to this compound containing uranium(VI) and copper(II) with bond-valence sums of 5.87, 6.03, 1.96, 2.16, and 1.86 being found for U(1), U(2), Cu(1), Cu(2), and Cu(3), respectively.[11,12]

Table 3. Selected Bond Distances (Angstroms) and Angles (Degrees) for $(UO_2)_2Cu(PO_3CH_2CO_2)(H_2O)_3$ **(UCuPAA-2)**

	Distances (Angstroms)		
U(1)−O(12)	1.775(5)	Cu(1)−O(9)	1.963(5)
U(1)−O(11)	1.781(4)	Cu(1)−O(15)	1.982(5)
U(1)−O(8)	2.261(4)	P(1)−O(3)	1.518(4)
U(1)−O(7)	2.277(4)	P(1)−O(2)	1.521(4)
U(1)−O(3)	2.316(4)	P(1)−O(1)	1.523(4)
U(1)−O(4)	2.462(5)	P(1)−C(1)	1.811(6)
U(1)−O(5)	2.682(5)	P(2)−O(8)	1.516(4)
U(2)−O(13)	1.783(4)	P(2)−O(7)	1.520(4)
U(2)−O(14)	1.776(4)	P(2)−O(6)	1.524(4)
U(2)−O(1)	2.283(4)	P(2)−C(3)	1.811(6)
U(2)−O(6)	2.303(4)	C(1)−C(2)	1.498(8)
U(2)−O(10)	2.341(4)	C(2)−O(4)	1.256(7)
U(2)−O(2)	2.374(4)	C(2)−O(5)	1.281(7)
U(2)−O(5)	2.558(4)	C(3)−C(4)	1.518(8)
Cu(1)−O(17)	1.949(5)	C(4)−O(9)	1.283(8)
Cu(1)−O(16)	1.954(5)	C(4)−O(10)	1.227(7)
	Angles (Degrees)		
O(12)−U(1)−O(11)	177.2(2)	O(16)−Cu(1)−O(9)	90.3(2)
O(14)−U(2)−O(13)	179.2(2)	O(17)−Cu(1)−O(15)	91.6(2)
O(17)−Cu(1)−O(16)	174.5(2)	O(16)−Cu(1)−O(15)	89.5(2)
O(17)−Cu(1)−O(9)	88.9(2)	O(9)−Cu(1)−O(15)	177.1(2)

Whereas the environment around the uranium(VI) ions is consistent between **UCuPAA-1**, **-2**, and **-3**, there is a remarkable change observed for the copper coordination in **UCuPAA-3**. Here, there are two roughly square planar CuO_4 groups containing Cu(1) and Cu(3) where all of the oxygen

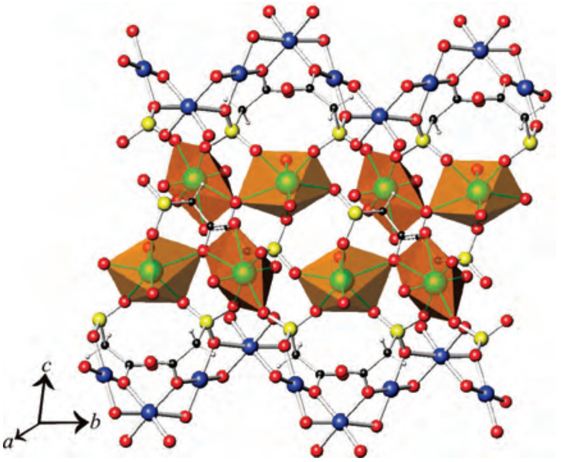

Figure 4. A view of the 3D anionic framework found for $[H_3O][(UO_2)_2Cu_2(PO_3CH_2CO_2)_3(H_2O)_2]$ (**UCuPAA-3**). UO_7 pentagonal bipyramids = orange, oxygen atoms = red, copper = blue, phosphorus = yellow, carbon = black, hydrogen = white. Disordered $[H_3O]^+$ cations have been omitted for clarity.

Table 4. Selected Bond Distances (Angstroms) and Angles (Degrees) for $[H_3O][(UO_2)_2Cu_2(PO_3CH_2CO_2)_3(H_2O)_2]$ **(UCuPAA-3)**

	Distances (Angstroms)		
U(1)−O(17)	1.771(9)	Cu(3)−O(8′)	1.925(9)
U(1)−O(16)	1.790(10)	Cu(3)−O(9)	2.006(9)
U(1)−O(11)	2.332(10)	Cu(3)-O(9′)	2.006(9)
U(1)−O(6)	2.335(9)	P(1)−O(1)	1.507(10)
U(1)−O(13)	2.362(9)	P(1)−O(2)	1.529(10)
U(1)−O(1)	2.363(9)	P(1)−O(3)	1.530(9)
U(1)−O(15)	2.654(10)	P(1)−C(1)	1.789(15)
U(2)−O(19)	1.778(10)	P(2)−O(6)	1.496(10)
U(2)−O(18)	1.780(10)	P(2)−O(8)	1.524(9)
U(2)−O(12)	2.243(10)	P(2)−O(7)	1.532(10)
U(2)−O(7)	2.304(9)	P(2)−C(3)	1.816(14)
U(2)−O(2)	2.308(9)	P(3)−O(12)	1.520(10)
U(2)−O(14)	2.448(10)	P(3)−O(13)	1.527(9)
U(2)−O(15)	2.614(9)	P(3)−O(11)	1.538(10)
Cu(1)−O(3)	1.902(9)	P(3)−C(5)	1.805(15)
Cu(1)−O(3′)	1.902(9)	C(1)−C(2)	1.52(2)
Cu(1)−O(5)	1.987(9)	C(2)−O(4)	1.230(18)
Cu(1)−O(5′)	1.987(9)	C(2)−O(5)	1.296(16)
Cu(2)−O(20)	1.948(10)	C(3)−C(4)	1.504(19)
Cu(2)−O(9′)	1.958(9)	C(4)−O(10)	1.226(18)
Cu(2)−O(5′)	2.009(5)	C(4)−O(9)	1.326(16)
Cu(2)−O(21)	2.031(11)	C(5)−C(6)	1.456(19)
Cu(2)−O(8′)	2.263(9)	C(6)−O(15)	1.287(15)
Cu(2)−O(3)	2.264(10)	C(6)−O(14)	1.297(18)
Cu(3)−O(8)	1.925(9)		
	Angles (Degrees)		
O(17)−U(1)−O(16)	177.9(5)	O(20)−Cu(2)−O(8)	89.8(4)
O(19)−U(2)−O(18)	177.9(5)	O(9′)−Cu(2)−O(8)	76.6(3)
O(3)−Cu(1)−O(3′)	180.0(2)	O(5)−Cu(2)−O(8)	106.7(4)
O(3)−Cu(1)−O(5′)	83.5(4)	O(21)−Cu(2)−O(8)	87.3(4)
O(3′)−Cu(1)−O(5′)	96.5(4)	O(20)−Cu(2)−O(3)	84.1(4)
O(5)−Cu(1)−O(5′)	179.999(1)	O(9′)−Cu(2)−O(3)	109.6(4)
O(3)−Cu(1)−O(5)	96.5(4)	O(5)−Cu(2)−O(3)	74.3(3)
O(3′)−Cu(1)−O(5)	83.5(4)	O(21)−Cu(2)−O(3)	92.3(4)
O(20)−Cu(2)−O(9′)	165.9(4)	O(8)−Cu(2)−O(3)	173.8(3)
O(20)−Cu(2)−O(5′)	92.6(4)	O(8)−Cu(3)−O(8′)	180.0(6)
O(20)−Cu(2)−O(9′)	165.9(4)	O(8)−Cu(3)−O(9)	96.2(4)
O(20)−Cu(2)−O(5)	92.6(4)	O(8′)−Cu(3)−O(9)	83.8(4)
O(9′)−Cu(2)−O(5′)	88.2(4)	O(8)−Cu(3)−O(9′)	83.8(4)
O(20)−Cu(2)−O(21)	93.2(5)	O(8′)−Cu(3)−O(9′)	96.2(4)
O(9′)−Cu(2)−O(21)	89.6(4)	O(9)−Cu(3)−O(9′)	179.999(2)
O(5)−Cu(2)−O(21)	164.8(4)		

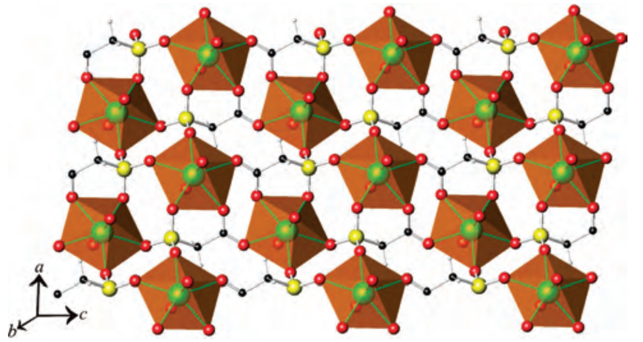

Figure 5. A depiction of the anionic layers found in $Na[UO_2(PO_3CH_2CO_2)]\cdot 2H_2O$ (**NaUPAA-1**). UO_7 pentagonal bipyramids = orange, oxygen atoms = red, phosphorus = yellow, carbon = black, hydrogen = white.

atoms are derived from the phosphonoacetate trianion. However, Cu(2) is found in a distorted octahedral environment. Part of this deviation from an idealized octahedral environment can be ascribed to a Jahn−Teller distortion, whereby there is an elongation of approximately 0.2 Å along a single axis of the octahedron. Two of the six oxygen sites in the CuO_6 unit are coordinated water molecules. These three copper(II) cations, along with sections of the phosphonoacetate, form 1D chains that extend along the *b* axis. These chains join the uranium-containing layers that extend in the [*ab*] plane. As found in **UCuPAA-2**, there are two distinct phosphonoacetate trianions. One of these is found exclusively in the uranium layers and simultaneously bonds to four uranium centers. The second phosphonoacetate uses its phosphonate portion to coordinate to two uranium centers and two copper sites. The carboxylate portion of this same anion is used exclusively to coordinate to two copper(II) ions with a single dangling oxygen atom being unused for metal bonding. The anionic charge in the framework is compensated for by disordered $[H_3O]^+$ cations. Selected bond distances and angles for **UCuPAA-3** can be found in Table 4.

Structure of $Na[UO_2(PO_3CH_2CO_2)]\cdot 2H_2O$ (NaUPAA-1). The structure of **NaUPAA-1** differs substantially from that of the copper containing compounds; although it is layered like **UCuPAA-2** and many other uranyl solids. Here, the uranium centers are found as isolated UO_7 pentagonal bipyramids. U═O bond lengths are quite normal at 1.779(4) and 1.773(4) Å, and U−O equatorial bonds range from 2.314(3) to 2.442(4) Å. The bond-valence sum for the single uranium center in **NaUPAA-1** is 5.98, which is consistent with this compound containing uranium(VI) again.[11] A view of part of one of the layers in the [*ac*] plane of this compound is shown in Figure 5. As can be seen from this figure, the phosphonoacetate ligand binds to four uranyl moieties and acts as both a chelating and bridging ligand.

The sodium cations play an interesting role in this compound in that they stitch the anionic layers together. This is quite common in uranyl compounds.[13] Here, they are found interacting with the uranyl oxygen atoms with a rather short contact of 2.538(5) Å. This sort of interaction is more

---

(13) Burns, P. C.; Miller, M. L.; Ewing, R. C. *Can. Mineral.* **1996**, *34*, 845. Burns, P. C. In *Uranium: Mineralogy, Geochemistry and the Environment*; Burns, P. C., Finch, R., Eds.; Mineralogical Society of America: Washington, DC, 1999; Ch. 1. Burns, P. C. *Mater. Res. Soc. Symp. Proc.* **2004**, *802*, 89. Burns, P. C. *Can. Mineral* **2005**, *43*, 1839.

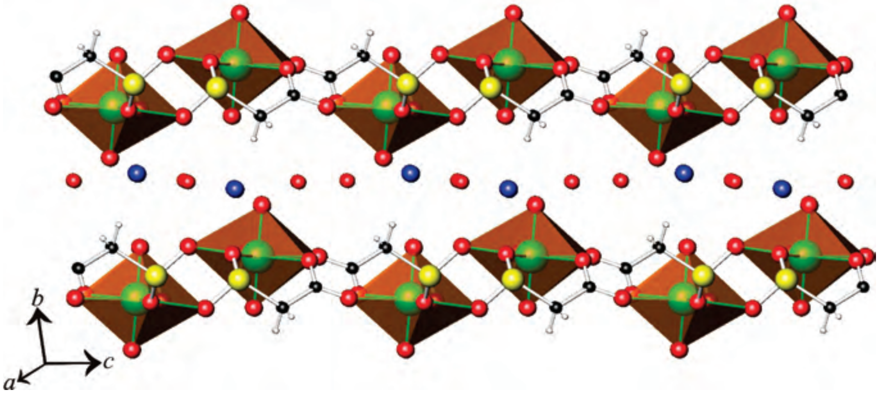

Figure 6. A view of the stacking of the anionic layers in $Na[UO_2(PO_3CH_2CO_2)]\cdot 2H_2O$ (**NaUPAA-1**) with Na^+ cations and water molecules between the layers. UO_7 pentagonal bipyramids = orange, oxygen atoms = red, sodium = blue, phosphorus = yellow, carbon = black, hydrogen = white.

Table 5. Selected Bond Distances (Å) and Angles (deg) for $Na[UO_2(PO_3CH_2CO_2)]\cdot 2H_2O$ (**NaUPAA-1**)

Distances (Angstroms)			
U(1)−O(6)	1.773(4)	P(1)−C(1)	1.809(5)
U(1)−O(7)	1.779(4)	C(1)−C(2)	1.517(7)
U(1)−O(2)	2.314(3)	C(2)−O(4)	1.256(6)
U(1)−O(3)	2.339(4)	C(2)−O(5)	1.262(6)
U(1)−O(1)	2.404(3)	Na(1)−O(8)	2.265(5)
U(1)−O(5)	2.408(4)	Na(1)−O(9)	2.351(4)
U(1)−O(4)	2.442(4)	Na(1)−O(9)	2.352(5)
P(1)−O(3)	1.520(4)	Na(1)−O(3)	2.494(4)
P(1)−O(2)	1.527(4)	Na(1)−O(7)	2.538(5)
P(1)−O(1)	1.537(4)	Na(1)−O(2)	2.587(4)
Angles (Degrees)			
O(6)−U(1)−O(7)	178.33(16)		

common in AnO_2^+ compounds that contain actinides in the +5 oxidation state, with $A_3AnO_2(CO_3)_2$ (A = Na, K, Rb; An = Np, Pu, Am) phases serving as prime examples of this.[14] A depiction of the stacking of the layers with interlayer Na^+ cations and water molecules is shown in Figure 6. The Na^+ cations are six-coordinate with a geometry that is highly distorted away from either an octahedron or a trigonal prism. Selected bond distances and angles for **NaUPAA-1** can be found in Table 5.

Fluorescence Spectroscopy. The fluorescence of uranyl compounds has been the subject of intense interest for many decades. In fact, the term fluorescence was coined in the late 1700s to describe the unusual green glow emitted from some uranium(VI) compounds when they are irradiated with long-wavelength UV light. The most characteristic feature of uranyl fluorescence is the fine-structure,[15–18] which can also be observed in the absorption mode. The fluorescence spectra of $UO_2Cu(PO_3CH_2CO_2)(OH)(H_2O)_2$ (**UCuPAA-1**), $(UO_2)_2Cu(PO_3CH_2CO_2)_2(H_2O)_3$ (**UCuPAA-2**), $[H_3O][(UO_2)_2Cu_2(PO_3CH_2CO_2)_3(H_2O)_2$ (**UCuPAA-3**), and $Na[UO_2(PO_3CH_2CO_2)]\cdot 2H_2O$ (**NaUPAA-1**) were collected from single crystals. In **UCuPAA-1**, **-2**, and **-3**, very weak emission is observed, and much of the fine structure is lost, as has been found in some uranyl fluorides[18] and more recently in silver uranyl phosphates.[19] In contrast, the emission from **NaUPAA-1** on a relative scale is intense, although the fine structure is still absent. The obvious difference between these compounds is the presence of copper(II), which has been previously noted to quench fluorescence in general and specifically in heterobimetallic uranyl/copper(II) compounds.[20]

Raman Spectroscopy. Analyses of $UO_2Cu(PO_3CH_2CO_2)(OH)(H_2O)_2$ (**UCuPAA-1**), $(UO_2)_2Cu(PO_3CH_2CO_2)_2(H_2O)_3$ (**UCuPAA-2**), $[H_3O][(UO_2)_2Cu_2(PO_3CH_2CO_2)_3(H_2O)_2$ (**UCuPAA-3**), and $Na[UO_2(PO_3CH_2CO_2)]\cdot 3H_2O$ (**NaUPAA-1**) using Raman spectroscopy were preformed to evaluate and compare several common vibrational modes in these compounds. The ν_1 symmetric stretching mode of the uranyl, UO_2^{2+}, cation in these compounds is found between 821 and 834 cm^{-1}.[21] The various stretching modes of the phosphonate moiety are located between 941 and 1053 cm^{-1}.[22] The carboxylate portion of the phosphonoacetate is found to exhibit stretching modes at approximately 1380 and 1520 cm^{-1}, as well as a deformation mode at 650 cm^{-1}.[23] The various U−O and Cu−O stretching modes as well as deformation modes found beneath 300 cm^{-1} are too convoluted to be assigned.

Conclusions

Mild hydrothermal conditions provide a convenient route for synthesizing and crystallizing heterobimetallic urani-

---

(14) Volkov, Y. F.; Kapshukov, I. I.; Visyashcheva, G. I.; Yakovlev, G. N. *Radiokhimiya* **1974**, *16*, 863. Simakin, G. A.; Volkov, Y. F.; Visyashcheva, G. I.; Kapshukov, I. I.; Baklanova, P. F.; Yakovlev, G. N. *Radiokhimiya* **1974**, *16*, 859. Volkov, Y. F.; Visyashcheva, G. I.; Tomilin, S. V.; Kapshukov, I. I.; Rukov, A. G. *Radiokhimiya* **1981**, *23*, 248.

(15) Carnall, W. T.; Crosswhite, H. M. In *The Chemistry of the Actinide Elements*; Katz, J. J., Seaborg, G. T., Morss, J. R., Eds.; Chapman and Hall: London, 1986; Ch. 16.

(16) Denning, R. G.; Norris, J. O. W.; Short, I. G.; Snellgrove, T. R.; Woodwark, D. R. In *Lanthanide and Actinide Chemistry and Spectroscopy*, ACS Symposium Series no. 131, Edelstein, N. M., Ed.; American Chemical Society, Washington, DC, 1980; Ch. 15.

(17) Grohol, D.; Clearfield, A. *J. Am. Chem. Soc.* **1997**, *119*, 4662.

(18) Almond, P. M.; Talley, C. E.; Bean, A. C.; Peper, S. M.; Albrecht-Schmitt, T. E. *J. Solid State Chem.* **2000**, *154*, 635.

(19) Yu, Y.; Zhan, W.; Albrecht-Schmitt, T E. *Inorg. Chem.* **2007**, *46*, 10214.

(20) Frisch, M.; Cahill, C. L. *Dalton Trans.* **2006**, *39*, 4679. Cahill, C. L.; de Lill, D. T.; Frisch, M. *CrystEngComm.* **2007**, *9*, 15. Fujiwara, M.; Wakita, H.; Matsushita, T.; Shono, T. *Anal. Sci.* **1991**, *7*, 483. Jay, J.; Johnston, L. J.; Scaiano, J. C. *Chem. Phys. Lett.* **1988**, *148*, 517. Ballard, R. E. *J. Chem. Soc.* **1965**, *3*, 2084.

(21) Frost, R. L.; Cejka, J.; Ayoko, G. A.; Weier, M. *Spectrochim. Acta, Part A* **2007**, *66A*, 979.

(22) Van der Veken, B. J.; Herman, M. A. *J. Mol. Struct.* **1975**, *28*, 371.

(23) Desseyn, H. O.; Van der Veken, B. J.; Aarts, A. J.; Herman, M. A. *J. Mol. Struct.* **1980**, *63*, 13.

um(VI)/copper(II) phosphonoacetate compounds. These are the first compounds of this type and point to a rich chemistry filled with new topologies and bonding modes. One of the structural trends that we are starting to observe in these phases is that the phosphonate portion of the anion is used preferentially for bonding to uranium; whereas it is more common to find the carboxylate moiety involved in coordinating the copper(II). This structural trend is consistent with the basicity of the different functional groups of phosphonoacetate, where the phosphonate unit is expected to be more basic, and to bond more strongly to a harder metal center like uranium(VI) than to a softer one like copper(II).[20,24] Whereas this work is in its early stages in terms of representing the general class of 5f−3d phosphonate compounds, one weakness is obvious − the difficulty of obtaining pure phases that will allow for further physical property measurements. There are a number of possible solutions to this conundrum, the most obvious one of which is to use a transition metal with a more fixed geometry, like iridium(III). However, to realize the possibility of developing magnetostructural correlations, it will most likely be necessary to carefully tune this chemistry with flexible paramagnetic first-row transition metals like copper(II). All of this will need to be elucidated before the replacement of a uranyl group by a neptunyl group can occur. For example, in **UCuPAA-1** there are two bridging oxygen atoms between the uranium and copper centers, allowing for the possibility of a superexchange if there were unpaired electrons on the actinide ion. What is envisioned for the future should now be obvious − a structure like **UCuPAA-1** where the uranium(VI) ($5f^0$) has been replaced by neptunium(VI) ($5f^1$).

Acknowledgment. This work was supported by the Chemical Sciences, Geosciences and Biosciences Division, Office of Basic Energy Sciences, Office of Science, Heavy Elements Program, U.S. Department of Energy under grant DE-FG02-01ER15187.

Supporting Information Available: X-ray crystallographic files in CIF format for $UO_2Cu(PO_3CH_2CO_2)(OH)(H_2O)_2$ (**UCuPAA-1**), $(UO_2)_2Cu(PO_3CH_2CO_2)_2(H_2O)_3$ (**UCuPAA-2**), $[H_3O][(UO_2)_2Cu_2(PO_3CH_2CO_2)_3(H_2O)_2$ (**UCuPAA-3**), and $Na[UO_2(PO_3CH_2CO_2)]\cdot 3H_2O$ (**NaUPAA-1**). This material is available free of charge via the Internet at http://pubs.acs.org.

IC800192R

---

(24) Nash, K. L. *J. Alloys Compd.* **1997**, *249*, 33. Jensen, M. P.; Beitz, J. V.; Rogers, R. D.; Nash, K. L. *J. Chem. Soc., Dalton Trans.* **2000**, *18*, 3058.